Numerical modelling of the volcanic plume dispersion from the hydrothermal system of La Soufrière de Guadeloupe

Yuly Paola Rave Bonilla, David Jessop, Séverine Moune, Céline Garbin, Roberto Moretti

RESEARCH ARTICLE

VOLCANICA

Numerical modelling of the volcanic plume dispersion from the hydrothermal system of La Soufrière de Guadeloupe

Yuly Paola Rave-Bonilla[α,β], David E. Jessop*[α,γ], Séverine Moune[α,γ], Céline Garbin[δ], and Roberto Moretti[ε]

[α] Université Clermont Auvergne, CNRS, IRD, OPGC, Laboratoire Magmas et Volcans, F-63000 Clermont-Ferrand, France.
[β] School of Geosciences, University of South Florida, Tampa, FL, USA.
[γ] Université de Paris Cité, Institut de physique du globe de Paris, UMR 7154 CNRS, 1 rue Jussieu, F-75238 Paris, France.
[δ] Gwad'Air - Air Quality Monitoring Agency, 97170 Petit-Bourg, France.
[ε] Università della Campania "L. Vanvitelli" Dip. Ingegneria, Via Roma 29, 81031 Aversa (I), Italy.

Abstract

Passive volcanic degassing results in the emission of toxic gases such as H_2S at quasi-steady rates over long periods that pose a significant hazard to human health even in low gas concentrations. Currently, La Soufrière de Guadeloupe has one of the highest gas emission rates in the Lesser Antilles arc, with gas emitted mainly from low-temperature fumaroles. In this study, gas dispersion from the volcano between 2016 and 2021 was modelled using a numerical code that takes into account wind and atmospheric data, topography, and gas flux measurements. We ran c.100 individual simulations of the most frequently observed wind and gas flux conditions using a Monte Carlo scheme. Our results, validated using air-quality measurements and citizen-science surveys, show that the most exposed zones are the hamlet of Matouba and the upper St. Claude. These areas have a 20 % and a 5 % probability, respectively, of exceeding H_2S guidelines for long-term gas exposure (70 ppb).

Résumé

Le dégazage volcanique passif émet des gaz toxiques tels que l'H_2S sur de longues périodes, ce qui représente un risque important pour la santé, même pour des faibles teneurs en gaz. Actuellement, La Soufrière de Guadeloupe émet des flux de gaz les plus élevés de l'arc des Petites Antilles, via des fumerolles de basses températures. Ici, nous étudions la dispersion des gaz de ce volcan entre 2016 et 2021 via la modélisation numérique en prenant en compte les données atmosphériques, la topographie et les mesures de flux de gaz. C.100 simulations ont été effectuées avec les conditions le plus fréquement observées. Nos résultats, validés par des mesures de qualité de l'air et par des retours de citoyens, suggèrent que les zones les plus exposées sont le hameau de Matouba et les hauteurs de Saint-Claude où il y a respectivement 20 % et 5 % de probabilité de dépasser les recommandations pour l'exposition long-terme à l'H_2S (70 ppb).

Keywords: Volcanic gas dispersion; Numerical modelling; Exposure map; Monte Carlo simulation; Long-term exposure; Citizen science.

Submitted: 2022-12-11 | Accepted: 2023-09-26 | Published: 2023-11-28

Editor: C. Montagna | Typesetter: J. Farquharson

1 Introduction

A common aspect of the activity at most volcanic edifices is volcanic degassing. In many dormant volcanoes, the supply of volatiles and heat from the magma reservoir to shallow aquifers [Rye et al. 1992; Giggenbach 1996; Rye 2005; Fischer and Chiodini 2015] maintains a hydrothermal system within the volcanic edifice [Christenson et al. 2010]. A well-developed hydrothermal system with persistent surface manifestations is often generated in tropical-climate rainfall regimes owing to the coexistence of abundant groundwater and an active magma reservoir [Fischer and Chiodini 2015]. Millions of people are then potentially exposed to volcanic gases worldwide, and exposures may differ from those in anthropogenic air pollution. The chemical composition of volcanic gases is controlled by the mixture of volatile components that are generated by shallow magmatic degassing. The main compounds found in volcanic gases are CO_2 (1–40 %), volatile sulphur compounds (SO_2, 1–25 %, H_2S, 1–10 %) and halogens (e.g. HCl, 1–10 %) [Textor et al. 2004]. In closed-conduit volcanoes, H_2O may represent more than 90 % [Aiuppa 2005; Oppenheimer et al. 2011; Moretti et al. 2013]. The interaction of magmatic gases with groundwater of a hydrothermal system produces degassing manifestations enriched in steam and less soluble gases such as CO_2, H_2S, H_2, CH_4, and CO [Symonds et al. 2001]. Exposure to these compounds has been the cause of the majority of volcanic gas-related pathologies [e.g. breathing difficulties; Beauchamp et al. 1984; Baxter et al. 1990; WHO 2000; Guidotti 2010] and fatalities [Williams-Jones and Rymer 2015]. Moreover, persistent volatile degassing, known as passive degassing, can be as harmful as sporadic effusive/explosive eruptions [D'Alessandro 2006; Oppenheimer et al. 2011; Fischer and Chiodini 2015], especially for long-term (years to decades) degassing. Indeed, long-term exposure to plumes generated by passive degassing and/or fumarolic emissions has a general impact on vegetation, especially crops [Baxter et al. 1982; Tortini et al. 2017], and on human health, even at very low concentration < 1 ppm) [ATSDR 1999; CalOEHHA 2000; U.S. EPA 2003]. Therefore, quantitative hazard assessment focused on volcanic plume dispersion for high exposure zones is a necessary and valuable tool for adequately understanding the health risks associated with long-term exposure to volcanic gas emissions [Pareschi et al. 1999].

* d.jessop@opgc.fr

Through numerical simulations, this study investigated volcanic gas dispersal from La Soufrière de Guadeloupe and the associated hazards posed to local populations. These are based on typical wind regimes and the patterns of gas dispersion that result from the gas fluxes and concentrations recorded from 2016–2021. We calculated the most probable gas dispersion scenario from La Soufrière volcano from the average of all simulated concentration maps, and also the probability of exceeding derived exposure guidelines by the World Health Organization (WHO), the Agency for Toxic Substances and Disease Registry, the California Office of Environmental Health Hazard Assessment, and the U.S. Environmental Protection Agency.

2 Volcanic and geologic context

La Soufrière de Guadeloupe volcano (16.0446° N, 61.6642° W, 1467 m a.s.l) is located in the central region of the Lesser Antilles, a volcanic arc formed by the subduction zone of the North American plate under the Caribbean plate [Feuillet et al. 2002]. La Soufrière is an andesitic dome-forming volcano considered the youngest edifice of the Grande Découverte complex (445 ka), formed during the last magmatic eruption in c. 1530 CE [Boudon et al. 2008]. It is among the most active and potentially deadly volcanoes of the Lesser Antilles arc [Komorowski et al. 2005]. This volcano is situated within the Basse-Terre urban unit whose population is approximately 50,000 inhabitants. Several communes, such as Matouba (~3500 inhabitants), St. Claude (~10,500 inhabitants), and Basse-Terre are located on the south and southwest slopes of the volcano only 5 to 10 km from the actively degassing fumaroles (Figure 1).

Since its last magmatic eruption in 1530 CE, the eruptive activity of La Soufrière has been mainly hydrothermal, with several phases of intense explosive hydrothermal or non-magmatic phreatic eruptions, plus the formation of fumaroles, steaming ground, and hot springs [Komorowski et al. 2005]. Since 1992, La Soufrière has been in a phase of unrest involving seismic and fumarolic activity, after at least a decade of posteruptive quiescence [Komorowski et al. 2005; Allard et al. 2014; Tamburello et al. 2019; Moretti et al. 2020; Jessop et al. 2021]. The peak of activity was recorded in April 2018, characterised by a volcano-tectonic (VT) earthquake (M_L 4.1) that marked the onset of a seismic swarm and an increase of summit fumarolic activity, with a maximum temperature of 111.4 ° C and gas exit velocity of 80 m s^{-1} [Moretti et al. 2020].

Transfer of heat and gases from the magmatic mush [7–9 km b.s.l.; Metcalfe et al. 2021] to the hydrothermal system of La Soufrière maintains persistent hydrothermal activity [Feuillard et al. 1983; Allard et al. 2014]. Summit fumaroles, where vent temperatures vary from 96 to 110 ° C [Allard et al. 2014; Moretti et al. 2020; Jessop et al. 2021], result from the rise of magma-derived gases through deep fractures in the basement interacting with shallow aquifers. In turn, these aquifers are sustained by the tropical climate, with typical annual rainfall of 7–10 m yr^{-1} [Moretti et al. 2021; OVSG-IPGP 1999–2022]. The magmatic gases mix with hydrothermal fluids and reach the surface at the summit through permeable fractures that cut through the lava dome [Moretti et al. 2020].

The summit vents are located in vertically permeable zones near major faults and fractures [Komorowski et al. 2005]. The most active fumarolic vent of La Soufrière is Crátere Sud (CS, an alignment of three separate but closely spaced vents) which yields a total dry gas flux of around 4.2 t d^{-1} [Allard et al. 2014; Jessop et al. 2021; Moune et al. 2022]. Two other main active fumaroles Gouffre-56 (G56) and Tarissan (TAS) have lower fluxes (about 2.4 t d^{-1} and 4 t d^{-1}, respectively [Jessop et al. 2021; Moune et al. 2022]). Napoléon Est (NapE) and Napoléon Nord (NapN) are vents that have opened as recently as 2014 (Figure 1) but with much lower fluxes [OVSG-IPGP 1999–2022].

The fumarolic gas composition, measured by MultiGAS from 2012 to 2021, shows a prevalence of water vapour that varies in the range of 86–98 %. The dry gas is mainly composed of CO_2 (74 mol.%) and H_2S (24 mol.%) and SO_2 (0.7 mol.% [Allard et al. 2014; Tamburello et al. 2019; Moune et al. 2022]). Summit emissions consist of 20 to 75 t d^{-1} of H_2O, up to 15 t d^{-1} of CO_2, and H_2S from 1 to 4 t d^{-1} [Allard et al. 2014; Tamburello et al. 2019; Moune et al. 2022]. The total heat flux of the fumarolic field was estimated in 2020 at 28.3 ± 6.8 MW, accounting for 77.5 % of the total heat output of the volcano besides the ground and thermal springs [Jessop et al. 2021]. Gas emissions at the current level of activity of La Soufrière could thus present a hazard for tourists, park operators and scientists, as well as for the thousands of people living in its proximity.

3 Methods

3.1 Numerical model

3.1.1 *Choice of numerical model*

The dispersion of volcanic gases in plumes is governed by gravity, wind strength, atmospheric turbulence, and stability [Cortis and Oldenburg 2009; Costa and Macedonio 2016]. When the density difference between plume and atmosphere is large, gravitational dispersion dominates whereas turbulent dispersion dominates for low density differences. These effects are encapsulated in the Richardson number,

$$\mathrm{Ri} = \frac{1}{w^2}\left(\frac{g'q}{R}\right)^{2/3}, \qquad (1)$$

where g' is the reduced gravitational acceleration due to density differences [Turner 1979], q is the volumetric flow rate of the plume, R is the plume radius, and w is the wind velocity at the reference altitude. Gas transport is considered as essentially passive (i.e. the plume is advected by the local wind field) when $\mathrm{Ri} < 0.25$ whereas when $\mathrm{Ri} > 1$ density plays a substantial role in driving the motion of the plume [Cortis and Oldenburg 2009; Costa and Macedonio 2016]. Thus, for small Ri, we may neglect the influence of gas concentration on density and hence gravitational motion, thereby simplifying the modelling process. Gases currently emitted at La Soufrière volcano are generally close to atmospheric density (hence small g') whereas the wind speed is relatively large. This regime has essentially remained unchanged since the beginning of its

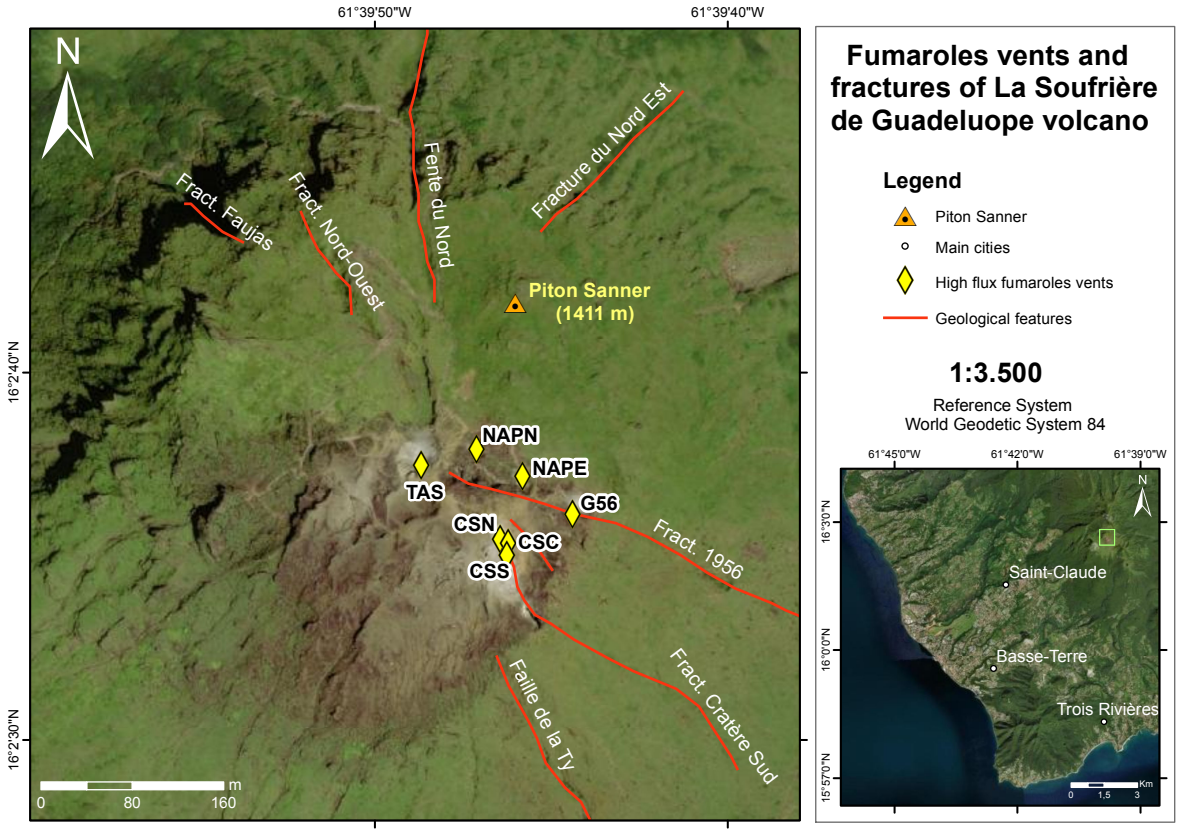

Figure 1: La Soufrière de Guadeloupe volcano location. Fumarolic vents and fractures in the summit of the volcano. Data from Komorowski et al. [2005] and ESRI.

unrest period in 1992. Using average gas compositions (H_2O, 95 mol.%; CO_2, 3 mol.%; H_2S, 2 mol.%), atmospheric temperature and pressure (18 ° C, 0.9 bar) and plume temperature (100 ° C), we obtain plume and atmospheric densities of 0.59 and 1.06 kg m^{-3}, respectively. Thus, for the wind-flattened plumes at la Soufrière where the plumes are typically 2–3 m thick [Allard et al. 2014; Tamburello et al. 2019], a total gas flux of 5 m^3 s^{-1} [Jessop et al. 2021; Moune et al. 2022], and range of wind speeds at the summit 1.3–22 m s^{-1} (Figure 3B) (calm to moderate conditions, Piton Sanner data IPGP-OVSG), we estimate Ri ≃ 0.0003–0.08 and conclude that passive degassing is a more than reasonable assumption for the current activity at La Soufrière. Consequently, the plume motion is entirely due to advection by the wind (i.e. plume speed and direction is identical to wind speed and direction). `DISGAS-2.0` (herein referred to as `DISGAS`) is an Eulerian numerical model for passive gas dispersion. It considers the gas to be a continuous medium in which transport is observed from a fixed point in a static coordinate system. It computes the spatial and temporal distribution of the gas concentration on a given domain or terrain model. Gas transport is calculated based on the solution of the advection-diffusion equation for a tracer gas of concentration C,

$$\frac{\partial C}{\partial t} + U\frac{\partial C}{\partial x} + V\frac{\partial C}{\partial y} + W\frac{\partial C}{\partial z} = \frac{\partial}{\partial x}\left(K_h\frac{\partial C}{\partial x}\right) + \frac{\partial}{\partial y}\left(K_h\frac{\partial C}{\partial y}\right) + \frac{\partial}{\partial z}\left(K_z\frac{\partial C}{\partial z}\right) + Q, \quad (2)$$

where t is time, x, y, and z are Cartesian (orthogonal) components of the space, and Q is the source term. Turbulent diffusion was assumed to be isotropic in the horizontal, and the diffusion coefficient, K_h, was parameterised using a Smagorinsky "large eddy" approach. The vertical diffusion coefficient, K_z, was parameterised using Monin-Obukhov similarity theory [Costa and Macedonio 2016]. The wind-speed components (U, V, W) are obtained from the mass-consistent (i.e. divergence-free) and terrain-following `DIAGNO` Diagnostic Wind Model (DWM) [Douglas et al. 1990; Costa and Macedonio 2016]. Equation 2 was solved using a second-order Lax-Wendroff scheme [e.g. Ewing and Wang 2001].

3.1.2 *Simulation setup*

In order to determine gas dispersion at La Soufrière, we ran 97 and 136 simulations at 5 m and 25 m resolution, respectively (1 simulation equates to 1 day, and we ran 1 simulation at each resolution), with the most frequently observed wind patterns over the 2016–2021 period. For each simulation, we considered daily atmospheric conditions (wind speed and wind direction), as well as bulk fumarolic emissions, terrain, and roughness models. Finally, we ran 4 additional cases for specific days where volcanic gas odours had been reported (see Section *3.1.3*).

The version of `DIAGNO` bundled with `DISGAS-2.0` has a maximum (horizontal) grid size of 350 × 350 pixels. We ran simulations at both 5 m and 25 m resolution. When simulations were run at 5 m resolution, they covered 1.75 × 1.75 km (Table 1), i.e. an area only just larger than the volcano. These

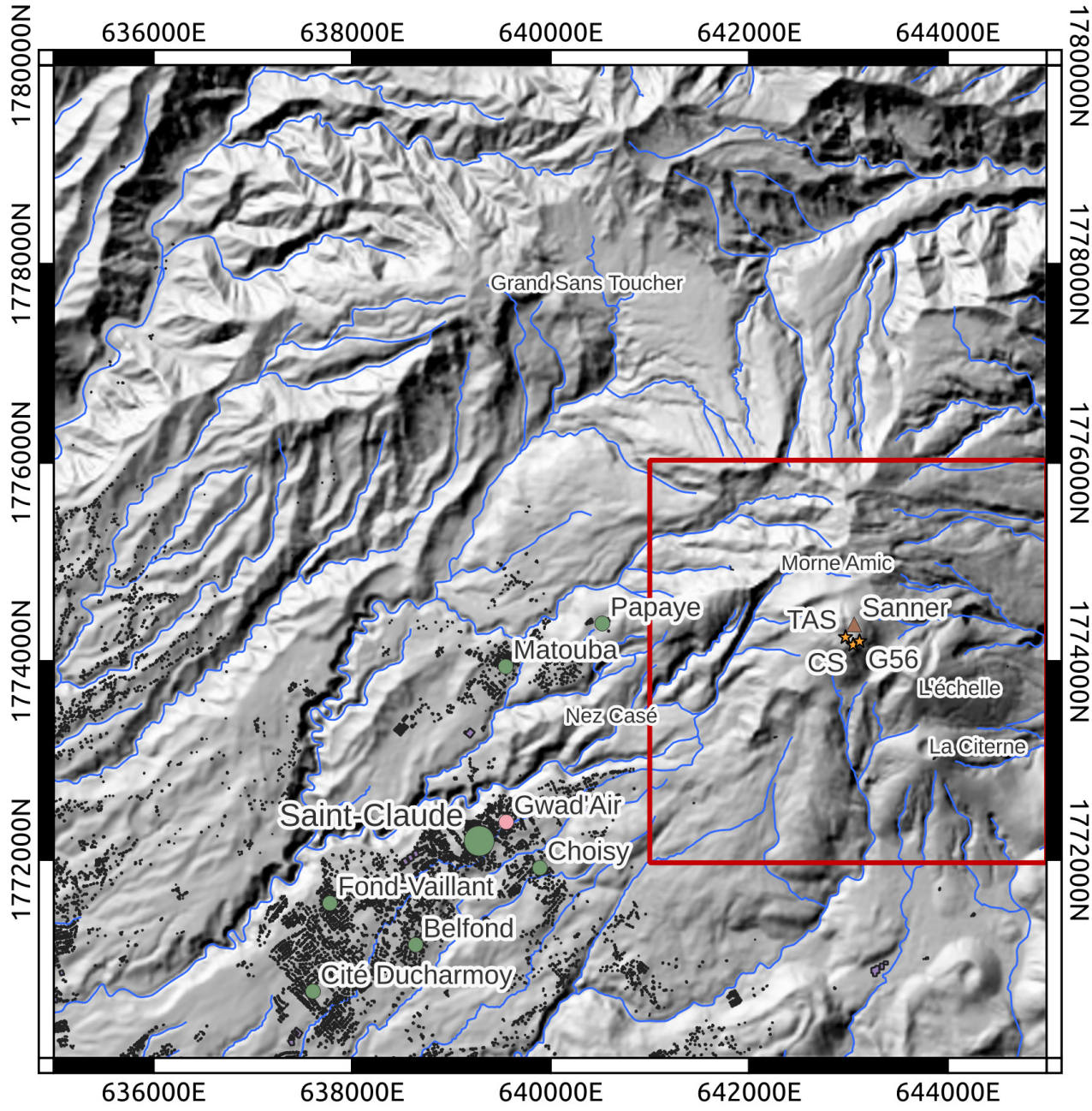

Figure 2: DEM used in our study from IGN LiDAR data (5 m resolution, WGS84 UTM20N). The red box shows the area covered by the 5 m resolution simulations. Dark squares indicate individual habitations, green circles show municipalities and orange stars show the locations of the fumaroles. Other place names, e.g. Morne Amic, are given in smaller font (no symbols).

high-resolution simulations were used to validate the results of the lower-resolution (25 m) simulations as well as to check the reproducibility of our results with those from Massaro et al. [2021]. At 25 m resolution, the area covered is 8.75 × 8.75 km (Figure 2). We saved the output four times per simulation (once every 6 hours), and each one of them had 14 layers going from the ground level until 110 m above it. Input files for both codes contain exactly the same setup details for all the simulated dates (Supplementary Material 1.A and Supplementary Material 1.B) and are adapted from the input codes from Massaro et al. [2021]. However, DIAGNO input files also contain atmospheric stability data, which are different for each day. Each simulation required approximately 24 h of computer time on a single processor, so our simulations were run in parallel using the supercomputer facilities of the Mésocentre Clermont Auvergne University.

3.1.3 *Specific cases*

An air quality (Gwad'Air) station was installed at the Roger Toumson Faculty of the Université Antilles-Guayane (16°01'37.9" N 61°41'44.1" W) in 2020. This station quantified H_2S and SO_2 concentrations with a detection limit of

Table 1: Input parameters used for DIAGNO and DISGAS 2.0 codes. These parameters apply for 5 m and 25 m resolution simulations, except for X and Y origins (Resolution means the distance covered by each cell).

Parameter	Input values	
	DIAGNO	DISGAS 2.0
X origin (5 m resolution)	642060	642060
Y origin (5 m resolution)	1773205	1773205
X origin (25 m resolution)	635623	635623
Y origin (25 m resolution)	1770627	1770627
X number of cells	350	350
Y number of cells	350	350
Z number of layers	14	14
Interval of time	From 00:00 to 23:00	Every 6 h from 00:00 to 24:00
Gas flux (CO_2) (CS)		0.0496 ± 0.0198 kg s^{-1}
Gas flux (CO_2) (G56)		0.0289 ± 0.0116 kg s^{-1}
Gas flux (CO_2) (TAS)		0.0347 ± 0.0139 kg s^{-1}

0.4 ppb for both gas species (approx. 0.39 and 0.72 ng m^{-3}, respectively). The relative errors on H_2S and SO_2 measurements are both approximately 5 %. Six different measurement campaigns were carried out between 14-06-2021 and 16-11-2021. Each month during this period, measurements were performed once per hour over the course of a week. The instrument was calibrated using a range of known concentrations for both H_2S and SO_2. Calibrations were performed before and after each campaign to avoid any potential instrumental drift.

The OVSG-IPGP has enabled an online survey for inhabitants around La Soufrière to report when they perceived odours related to volcanic gas emissions (such as fireworks for SO_2 or rotten egg for H_2S). Some reports were also made via the OVSG Facebook profile. The dates when people mentioned the presence of such odours were compared with the registered dates with the measured amounts of H_2S from the Gwad'Air air quality control station at St. Claude. We note that the perception of H_2S odours is not exclusively due to high gas concentrations and can be driven by favourable wind directions/speed. Nevertheless, as a check of coherence between the measured gases in the Gwad'Air station and the results from the numerical models we simulated only a restricted number of days (3) where high H_2S values were simultaneously recorded at the Gwad'Air station and reported in the online surveys. This allowed us to determine the gas concentration to which the St. Claude and Matouba populations can be exposed in such conditions.

3.2 Model inputs

3.2.1 *Meteorological data*

We selected days to be simulated from meteorological data dating from April 2016 to June 2019 from the Piton Sanner weather station (16.045° N, −61.662° E, 1411 m a.s.l., 05103 – 03 Campbell anemometer and wind vane at 2 m elevation, and Campbell PTB101B atmospheric barometer; see Figure 1 for the station location). We found the prevailing wind direction to be between 90° and 105° in azimuth (Figure 3A). Within this range of directions, we found that wind speed is most commonly between 11.1 and 16.6 m s^{-1} and approximately normally distributed (Figure 3B). Among those wind speed and direction ranges, we randomly selected dates to simulate using a Monte Carlo scheme and then obtained ECMWF-ERA5 reanalysis data (wind speed and direction, atmospheric pressure and lapse-rate at various atmospheric levels [Hersbach et al. 2020]) for each date, specified for 24 h of simulation. Finally, these data were preprocessed (wind speed and direction converted from polar to terrain- following cartesian components) and interpolated to the calculation grid using the PRESFC and PREUPR software [Douglas et al. 1990]. We note that, by using the ECMWF/ERA5-DIAGNO-DISGAS workflow, our approach is identical to that proposed by the VIGIL software [Massaro et al. 2021; Dioguardi et al. 2022; Viveiros et al. 2023].

3.2.2 *Gas fluxes*

Gas flux measurements were carried out approximately once a month between May 2016 to June 2021 [see Figure 3C, Supplementary Material 2.A; this work; Tamburello et al. 2019; Moune et al. 2022] by using a portable multi-sensor system (MultiGAS). This allows high frequency measurement of main gas compounds (CO_2, H_2S, SO_2) in volcanic plumes, as described in numerous studies [e.g. Aiuppa 2005; Shinohara 2005], including for La Soufrière [Allard et al. 2014; Tamburello et al. 2019; Moune et al. 2022]. To determine fumarolic gas fluxes from the three main vents where the fumarolic emissions are strong enough to generate a plume (CS, G56, TAS), we performed walking traverses orthogonal to the plume direction, a few metres downwind from the vents with the MultiGAS inlet at 0.9 and 2 m height [as described in Allard et al. 2014; Tamburello et al. 2019; Moune et al. 2022]. Most commonly, the fumarolic emissions were flattened to the ground by strong trade winds (up to 20 m s^{-1}), and their upper boundary stood at ca. 3–4 m above the ground with a maximum gas density centred at 1.5–2 m above the ground (our visual observations consistent with Gaudin et al. [2016] and Tamburello et al. [2019]).

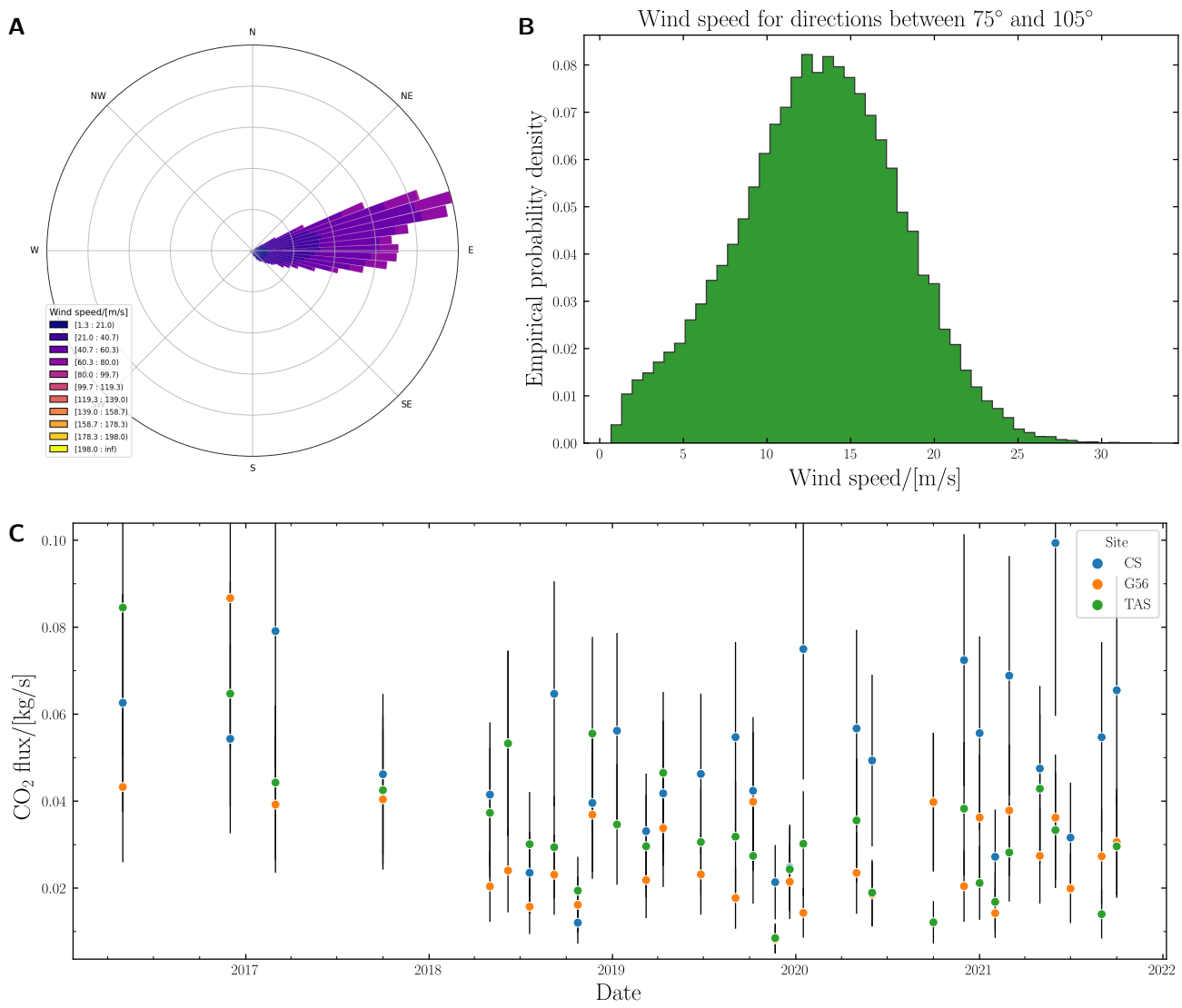

Figure 3: [A] Wind rose indicating the typical wind conditions in the top of La Soufrière (based on data from April 2016 to June 2021). Angular position indicates the direction from which the wind comes and radial extent of each sector indicates the frequency of each wind speed (see legend for values). [B] Wind speed distribution for winds coming from 090° to 105°. [C] CO_2 flux measured with MultiGas from the three main fumarole vents in the top of La Soufrière de Guadeloupe. Measurements from May 2016 to October 2021. Data from Tamburello et al. [2019], Moune et al. [2022], and this study.

Gas flux estimations were computed following Allard et al. [2014], Tamburello et al. [2019], and Moune et al. [2022]. We interpolated the concentration measurements using a 2D spline function and then integrated them over the plume cross section to obtain integrated concentration amounts (ICAs) using `RatioCalc` software [Tamburello 2015]. These computations were based on CO_2 as a volcanic marker, given that the IR CO_2 sensor reacts faster than the H_2S electrochemical sensor and CO_2 measurements are not affected by high humidity conditions [Tamburello et al. 2019]. Then, CO_2 fluxes were computed by scaling the obtained CO_2 concentration in plume cross sections with the average wind speed. Wind speed was measured with a portable anemometer at the same height as the MultiGAS inlet during all traverses. The major source of error in MultiGAS-estimated fluxes is wind speed uncertainty and we estimate that our gas flux relative standard error is of the order of 40 % [Tamburello et al. 2019].

We took the average CO_2 flux for the duration of the study period (2016 to 2021) for each of the sources as the gas flux input in our simulations. This is justified as, considering the relative standard error (40 %), the gas flux data do not show significant variation and we may thus consider them to be constant (Figure 3C). This is in keeping with Tamburello et al. [2019], who showed that CO_2 and H_2S fluxes do not change significantly over the scale of months or years (compared to gas flux estimation errors) if there is no drastic change in magmatic conditions, as is the case at La Soufrière. Thus we take the values of 0.0496 kg s^{-1} for CS; 0.0289 kg s^{-1} for G56, and 0.0347 kg s^{-1} for TAS as inputs for our simulations (see Table 1 and Supplementary Material 2.A).

Fumarolic gas fluxes were imposed in the simulations as point sources by writing the mass flow rate for each vent in a data file along with their geographical location and elevation above the terrain model. This file was then read by DISGAS at runtime and imposed on the nearest node of the computational domain [Costa and Macedonio 2016].

3.2.3 *Terrain models*

We used a 5 m resolution Digital Elevation Model obtained from the Institut Géographique National (IGN) airborne LiDAR datasets for topographic calculations in both DIAGNO and DISGAS. This was downsampled to 25 m for the corresponding simulations. We saw no significant effect of topographical resolution on our results, except in how well the wind fields were resolved which is consistent with Massaro et al. [2021]. Furthermore, the terrain surrounding La Soufrière consists of de-vegetated stony ground (summit and flanks of volcano), low-lying vegetation (flanks), tropical forest, and buildings and is evidently heterogeneous. In spite of this, we used a uniform terrain roughness of 0.5 m for all simulations, though we also tested uniform values of 0.05 and 5 m without significant impact to our results. The lack of difference is perhaps because the natural variation in terrain (i.e. orography) is much more important than surface roughness.

4 Results

4.1 Simulations

Simulations were run hourly, from 00:00 to 23:59, and had zero gas concentration throughout the computation domain at the start of each simulation. For visualisation and further analyses, we therefore use the gas concentration at the end of the day to ensure propagation of the simulated plume throughout the domain. We also selected the lowest layer, which covers from the ground level to 1 m above the ground level, as this corresponds to roughly the height at which people, plants and animals respire. We plot our simulation results in Figure 4, showing the ground-most layer for each of the simulations for both 5 m and 25 m resolutions. We note that the "speckle" seen in Figure 4 and Supplementary Material 2.B is numerical noise at the lowest concentration levels (~10^{-8} kg m^{-3}) so that, outside the plume, there is essentially no excess in simulated gas emissions.

We filtered the meteorological data for any corrupt files before simulations were run. The end result was a total of 97 simulations at 5 m resolution and 136 for 25 m resolution. Our simulations indicate variations in gas dispersion patterns from La Soufrière de Guadeloupe according to the variations in meteorological conditions. The predominant feature of our simulations is a westward gas propagation. The range of gas concentrations extends over 5 orders of magnitude, with the highest concentration achieved being between around 8×10^{-3} kg m^{-3} CO_2 and 5×10^{-3} kg m^{-3} CO_2, corresponding to 4440 and 2775 ppm CO_2 for the 5 m and 25 m resolution simulations, respectively (Figure 4). Note that these values refer to excess of atmospheric CO_2 concentrations, which is around 420 ppm at time of writing. The highest concentrations in each simulation are found close to the source. All simulations show a progressive decrease in gas concentration away from the source. In distal areas downwind of the volcano, the concentration is typically around 10^{-5} kg m^{-3} (5 to 6 ppm) CO_2.

In the 5 m resolution simulations, the plume has a straight trajectory without significant perturbations or changes of direction (Figure 4A). At least the first one to two kilometres travelled by the gases maintain the same trajectory that depends only on the atmospheric conditions of each day. This is expected due the short distance travelled (~1 km), which corresponds only to an area over the volcano. The initial straight trajectory is also observed in the 25 m resolution simulations, which cover an area of 8.75 × 8.75 km (Figure 4B). In many simulations, however, at around 2–3 km distance the plume changes trajectory by up to 45°, predominantly to the south.

4.2 Gwad'Air data and survey results

The results show that H_2S is the predominant sulphur species with a mean background concentration of about 11 µg m^{-3} and peak values between 40 and 62 µg m^{-3}. SO_2 was essentially at background concentration levels (~4 µg m^{-3}, Figure 5). Variations in background levels for both species are principally instrument noise with some variation due to day-to-day meteorological changes. According to these values (Figure 5), we can consider that the average ambient background air for SO_2 and H_2S is around 4 and 6 µg m^{-3}, respectively. To be more precise for H_2S, its background is around 5 µg m^{-3} for the first campaign, 3 µg m^{-3} for the second campaign, 0 µg m^{-3} for the third and the fourth campaigns, and 7 µg m^{-3} for the fifth and sixth campaigns. These background values have been removed from the dataset to obtain the real values of H_2S peaks.

A total of 28 reports of perceived odours related to volcanic degassing were filed with the OVSG by inhabitants of the towns surrounding La Soufrière, dating from September 2020 to the early 2022. Eighteen reports were made via online surveys, which were active in the second half of 2021. Ten additional comments were published on the OVSG Facebook page (Supplementary Material 2.D). The reported dates were compared with the Gwad'Air station data and we found three dates when the survey reports about sulphur odours coincided with the H_2S peaks measured at the air quality station, namely 15-06-2021, 07-10-2021, and 10-11-2021 (see Figure 5 and Supplementary Material 2.D).

5 Discussion

5.1 Typical gas dispersion patterns

From the individual simulations, we calculated average gas dispersion maps (Figure 6) (i.e. the empirical mean of all the data presented in Figure 4). This corresponds to the typical, or most probable, dispersion scenario and includes the inhabited areas closest to the volcano. We found that a minimum of 80 simulations was sufficient to achieve convergence of the mean concentration maps. The 5 m resolution dispersion map (Figure 6A) shows detail of the gas dispersion close to the volcano. We see the highest gas concentrations on the summit of the volcano close to the vents, and the initially westward propagation of the plume. Furthermore, we find the highest

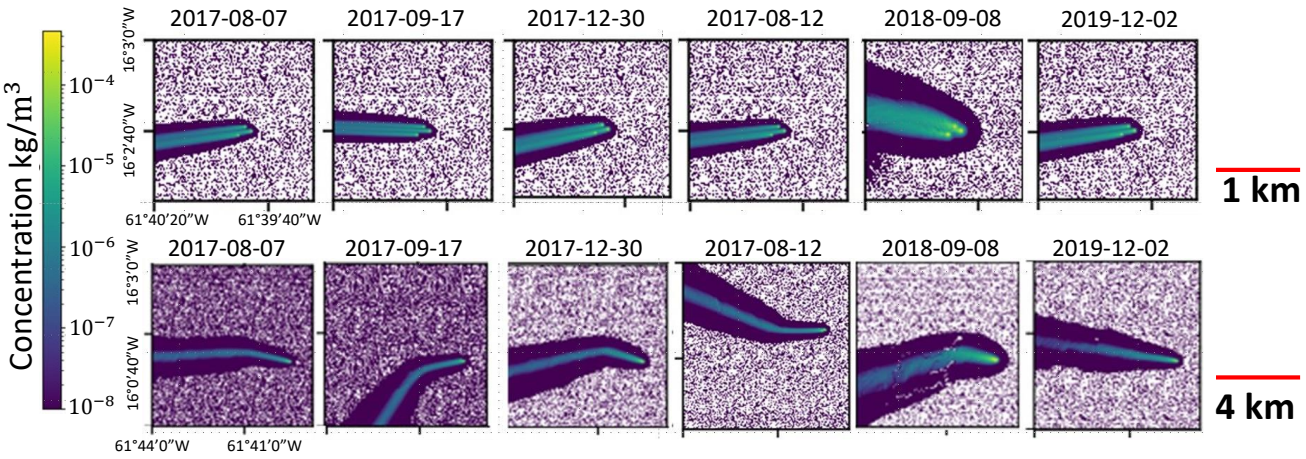

Figure 4: Examples of 5 m resolution (upper) and 25 m resolution simulations (lower) of CO_2 dispersion. Details of the individual simulations can be found in the supplementary material (Supplementary Material 2.B, Supplementary Material 2.C). The "speckle" seen in these figures is due to numerical noise at the lowest concentration levels. These figures represent the concen-

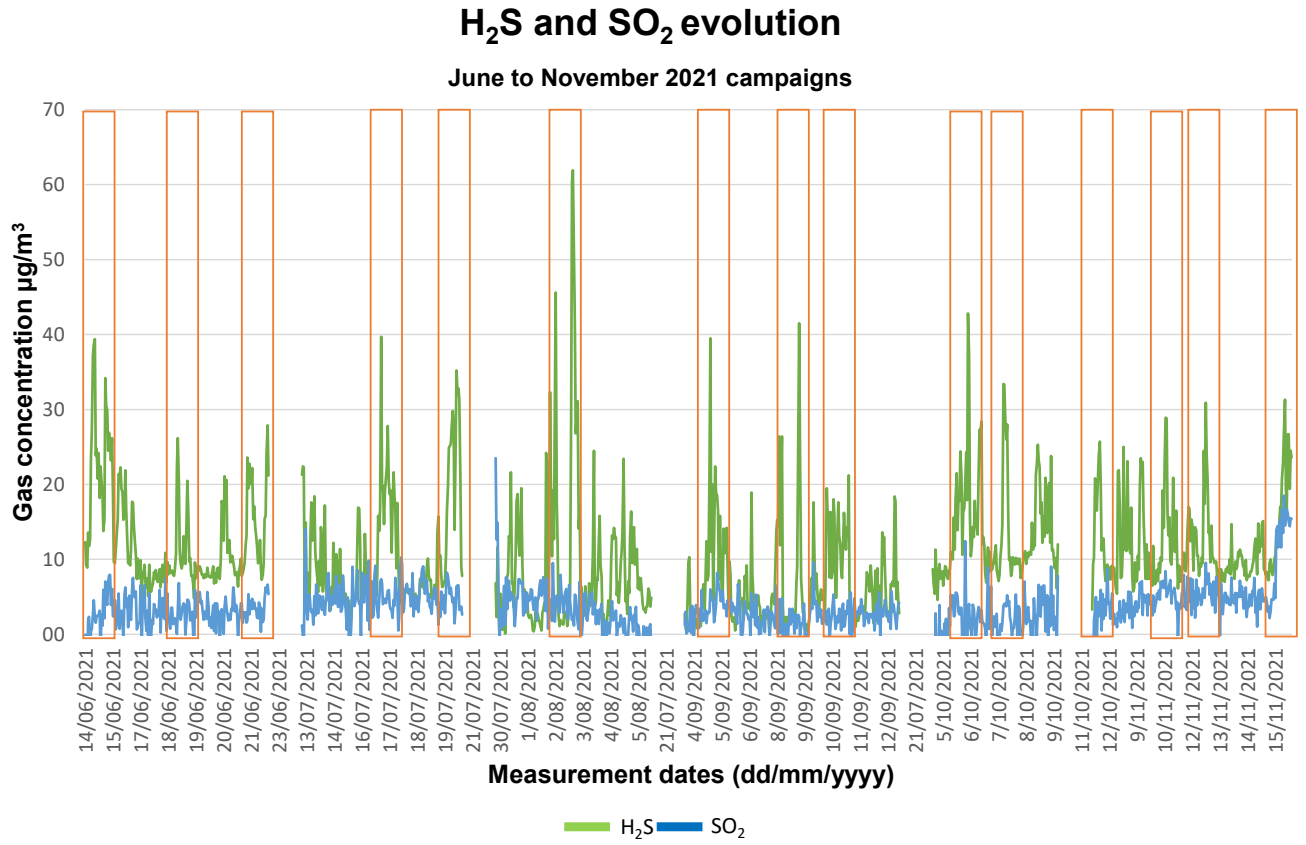

Figure 5: General H_2S and SO_2 evolution from June to November 2021. Data from Gwad'Air campaigns 1–6. Background is not removed. Orange rectangles highlight the H_2S peaks.

concentration of the gases in the core of the plume, around 8×10^{-3} kg m^{-3} CO_2 and rapidly decreasing to 10^{-5} kg m^{-3} CO_2 within 80 m of the source, i.e. still on the summit. Towards the edges of the plume, the gas concentration decreases more rapidly than in the core, decreasing to 10^{-7} kg m^{-3} CO_2 in less than 80 m from the vent. At 300 m from the vent, the concentration in the core decreases to around 10^{-7} kg m^{-3} as the plume flows down the western flank of the volcano.

In the average concentration map produced from the 25 m resolution simulations (Figure 6B), there is good agreement between this and the 5 m resolution dispersion map where these two overlap. The highest concentrations are still found

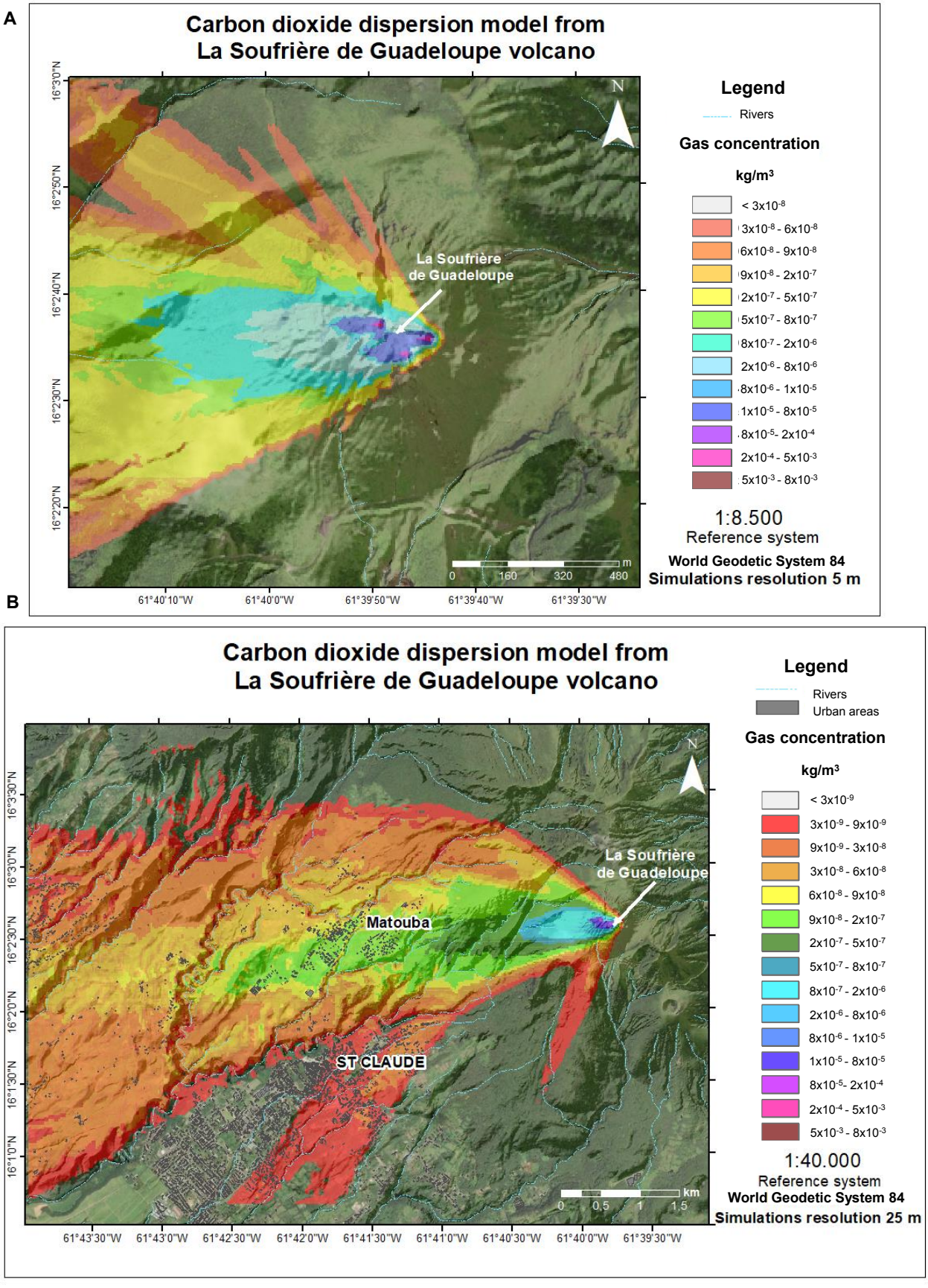

Figure 6: CO_2 dispersion model for the lower-most simulation layer (0–1 m) from La Soufrière de Guadeloupe based on [A] 5 m resolution simulation and [B] 25 m resolution simulations. Basemap from ESRI.

in the closest area to the vents, with CO_2 values around 8×10^{-3} kg m^{-3}. We observe the same westward dispersion and the highest concentrations are found at the core of the plume. At about 1 km from the vent (i.e. beyond the range of the 5 m simulations), the concentration at the core is about 10^{-7} kg m^{-3} CO_2. At around 1.5 km from the vent, the hamlet of Matouba experiences similar concentrations. The wind fields are strongly affected by the local topography, particularly the Grand Sans Toucher massif, which causes the plume to bentd southwards by about 2 km distance from the vent (see Figure 1 and Figure 2). In the farthest zones of our simulations we find the lowest gas concentrations, typically around 10^{-9} kg m^{-3} CO_2. We see approximately this level of concentration in the southern zone reaching the north-eastern and eastern parts of St. Claude. These are the closest areas of the town to La Soufrière, directly downwind of the volcano and at greater altitude than the rest of the town. In both model resolutions, the places where gas concentration and trajectory change coincide with elevated topographic features. In the 5 m resolution model, gas concentration decreases where the plume reaches the pronounced Morne Amic crater scar (see Figures 2 and 6A). It occurs after the first 500 m travelled in the main propagation direction and it happens again 300 m farther, in the northwestern side of the model. In these cases, the gas concentration decreases by one order of magnitude beyond the physical barriers. This behaviour is also visible in 25 m resolution simulations, where each time gas propagation finds a topographic protuberance, like those surrounding the dome in the northwestern sector of Figure 6B or the irregular relief in the north of the mapped zone, gas concentration decreases (Figure 6B). In the farthest zones from the volcano, gas concentration is lower in the leeward sides of the mountains, evidencing topography influence in gas dispersion behaviour.

Figure 6 shows that both model resolutions give similar results in terms of gas concentration, plume trajectory, and the effect of topography. Based on these results, the typical gas dispersion pattern is to the west, predominantly towards 260°. From these models we can establish that, in terms of population exposure to gas emissions, the most exposed town is Matouba (9×10^{-8} to 2×10^{-7} kg m^{-3} CO_2), followed by the north-east and eastern zones of St. Claude (9×10^{-9} to 3×10^{-8} kg m^{-3}) (Figure 6B).

5.2 Limitations of the numerical model

`DISGAS` has been used in several studies related to volcanic degassing, including Granieri et al. [2013], Pedone et al. [2017], and Massaro et al. [2021]. Notably, the latter carried out a study of degassing at La Soufrière similarly using gas fluxes obtained from MultiGAS traverses and Pitot tube measurements. They found that their simulation results showed similarity with measurements made by permanent MultiGAS stations situated close to the main vents despite a relatively low spatial resolution (15 m computational cells, but with 5 m and 25 m DEMs). We are hence confident that `DISGAS` is a useful modelling tool for gas dispersion at La Soufrière.

Our decision to run two sets of simulations at different resolutions was motivated by the necessity to extend the computational domain to St. Claude and beyond and in part, by the limitations in the computational domain inherent to `DIAGNO` (maximum of 350 × 350 cells in the horizontal plane). At 25 m resolution, we cover a sufficiently large physical area to incorporate these communities but, consequently, some detail on mixing and advection close to the vents is lost (Figure 6). As gas concentration and concentration gradients decrease rapidly with distance from the vent, resolution near the vent is critically important. Furthermore, the wind fields calculated in our simulations should also be strongly dependent on resolution, especially as La Soufrière and its surroundings have a complex orography with steep relief and deep, canyon-like valleys (Figure 2). The wind field will depend strongly on resolution especially at and around the summit where the variations in orography are greatest, and this dependence will diminish with distance from the summit. Furthermore, particularly for the 25 m resolution simulations, the mixing and dispersion processes near the vent are not directly modelled and instead rely on sub-grid scale parametrisations which may not capture them well. A spatially -variable resolution is not possible in `DISGAS-2.0`. Nevertheless, our 5 and 25 m resolution simulations are qualitatively similar in terms of the typical direction of dispersion and the concentrations seen at a given distance from the vents. This may be a consequence of the averaging procedure employed: though the details of a given simulation may be different between the different resolutions, on average we capture the essence of the plume motion and how gas concentration varies spatially.

`DISGAS` calculates the dispersion of a single passive gas tracer but there is no discrimination as to what gas can be used. For example, Massaro et al. [2021] considered H_2O as their tracer and prescribed vent fluxes as per the steam-flux calculations of Tamburello et al. [2019] and Jessop et al. [2021]. Here, we have used CO_2 as this species is conservative and thus is not underestimated by MultiGAS measurements [Jessop et al. 2021] so by default our predicted concentration of dispersed gas is reported as CO_2 concentration. All present gas species are assumed to passively advect together in the plume. Conversion from CO_2 fluxes to other species of interest, such as H_2S, was achieved using mass ratios determined from MultiGAS measurements at the summit (see Supplementary Material 2.A and Table 2).

5.3 Gas detection in nearby populations

5.3.1 *Air quality data*

Figure 5 indicates at least 15 dates with spikes in H_2S concentration. H_2S peaks were sporadic and no event resembled another, suggesting that they were due to non-atmospheric forcings, from volcanic degassing. Despite the oxidation of H_2S by molecular oxygen and hydroxyl radicals of air [Davis and Kirkland 1979] forming SO_2 and ultimately sulphates [Hill 1973], with a residence time in air typically <1 day, no correlation between an increase in SO_2 and a decrease in H_2S was observed. Indeed, SO_2 and sulphate compounds are removed from the atmosphere through absorption by waters, plants and soils, or wet precipitation [Williams-Jones and Rymer 2015] which is coherent with the lack of variation in SO_2 over background levels seen at St. Claude. We hence concentrate solely on the dispersion of H_2S.

Table 2: Inputs for survey date simulations with their respective H_2S concentration average measured by Gwad'Air (without background values) and the resulting simulated values for the places closest to the Gwad'Air station.

Date	H_2S flux from top (kg s^{-1}) average month	Wind speed (m s^{-1})	Wind direction (degrees)	H_2S Gwad'Air station (g m^{-3}) average per day (± error)	Closest H_2S simulated to the reported place (g m^{-3})	Closest H_2S simulated to the reported place (ppb)
15-06-21	0.0452	4.41	063°	19.80 (±0.99)	1–10	0.7–7
02-08-21	0.0269	3.1	079°	15.30 (±0.76)	1–10	0.7–7
07-10-21	0.038	5.14	079°	7.20 (±0.36)	1–10	0.7–7
10-11-21	0.0347	3.55	069°	4.80 (±0.24)	1–10	0.7–7

5.3.2 *Survey results*

The reported dates were compared with the Gwad'Air station data and we found three dates when the survey reports about sulphur odours coincided with the H_2S peaks measured at the air quality station, namely 15-06-2021, 07-10-2021, and 10-11-2021 (see Figure 6 and Supplementary Material 2.C). On 10-11-2021, H_2S odours were reported in Baillif, a community located 6 km downwind of the summit of La Soufrière. Therefore, we also considered it as a good example to compare the results of our simulations with the Gwad'Air measurements despite reports not emanating from St. Claude. We note that there are no survey reports from Matouba, despite its proximity to the volcano and frequent exposure to volcanic gases (Figure 6). This may be due to the principally rural condition of this hamlet, implying fewer inhabitants and less online activity.

We plot the hourly H_2S gas concentrations measured for those dates in Figure 7. By way of comparison, Figure 7 also shows the date with the highest H_2S peak (02-08-2021) though no reports were received on this date. We also did a simulation of it as a good example of high H_2S presence in St. Claude. The absence of reports may in part be due to it being the middle of the summer holidays, with many residents absent and incoming tourists unaware of the online surveys.

These results reveal that the H_2S peaks generally occur at night or later in the afternoon when temperatures are lower (Figure 7). However, ambient temperature variations from day to night around La Soufrière de Guadeloupe do not usually exceed 10 °C and seasonal meteorological changes just imply variations in the rain regime, which cannot generate H_2S peaks of > 30 µg m^{-3}. The H_2S peaks are not long-lasting and seem to be simply due to a higher H_2S flux at different times during these days, without a specific relationship with time.

5.3.3 *H_2S model simulations for specific dates*

In order to establish the relationship between the presence of gases such as H_2S in the towns near La Soufrière de Guadeloupe and the gas emissions from the volcano, we performed simulations of these specific days and compared the direction, extent of propagation and gas concentration resulting from the models with the Gwad'Air data (Figure 8). Simulations were started at 00:00 for each day: that is, the accumulation of emissions from previous days is not considered. We used the average H_2S fluxes from the corresponding month as input values for the gas flux (see Supplementary Material 2.A and Table 2).

As the survey report of 15-06-2021 indicates that the event started at 7:45 am, we needed to obtain the closest situation to the one that could occur in the early morning of 15th June. Therefore, we started the simulation in the latter hours of the previous day (14-06-2021). For that specific day, the dispersed gases reach the north-eastern sector of St. Claude, where the Gwad'Air station is located, and a few metres (< 1 km) from the Choisy sector named in the survey. According to the Gwad'Air measurements, the range of values of H_2S concentration that day was from 4.7 (± 0.23) to 21.2 (± 1.06) µg m^{-3}, with an average of 19.8 (± 0.99) µg m^{-3}. The simulated H_2S concentration for these locations is from 1 to 10 µg m^{-3} (Figure 8A) which differs just by around 10 µg m^{-3} from the average H_2S measured that day by the Gwad'Air station, which suggests a good concordance between both techniques (Table 2).

According to Figure 7, the three other selected dates present the highest H_2S concentrations at the end of the day. Therefore, we represented the resulting simulation of the final hour of each day, as we considered it the closest scenario to the real one. The highest H_2S recorded peak was on 02-08-2021. On this day, the simulated gas plume is noticeably broader than on other dates (Figure 7B). The plume reaches 300 m of St. Claude covers a broader area than the other simulations. If we compare input values for these simulations, we find that the only significant difference from this date to the three other cases, is wind speed (Table 2). On 02-08-2021 wind speed was 3.1 m s^{-1} (11.16 km h^{-1}), the lowest wind speed from the four cases, which shows that, under calm conditions, gases are dispersed over a wider area, though they may not extend far downwind in noticeable concentrations (>1 µg m^{-3} the lowest limit showed by our simulations). Regarding H_2S concentration, Gwad'Air measurement values for this date were from 1.1 (± 0.05) to 61.9 (± 3.09) µg m^{-3} with an average of 15.3 (± 0.76) µg m^{-3}. The simulated value is 1–10 µg m^{-3}, suggesting a difference of less than 6 µg m^{-3}.

For the two other selected cases, 07-10-2021 and 10-11-2021, the Gwad'Air H_2S concentration measurements ranged from 0 to 26.4 (± 1.32) µg m^{-3} with an average of 7.2 (± 0.36) µg m^{-3}, and from 0 to 21.9 (± 1.09) µg m^{-3} with an average of 4.8 (± 0.24) µg m^{-3} respectively (Table 2). In those cases, the simulated H_2S level closest to the Gwad'Air station was between 1 and 10 µg m^{-3} (Figure 8C–D), implying a dif-

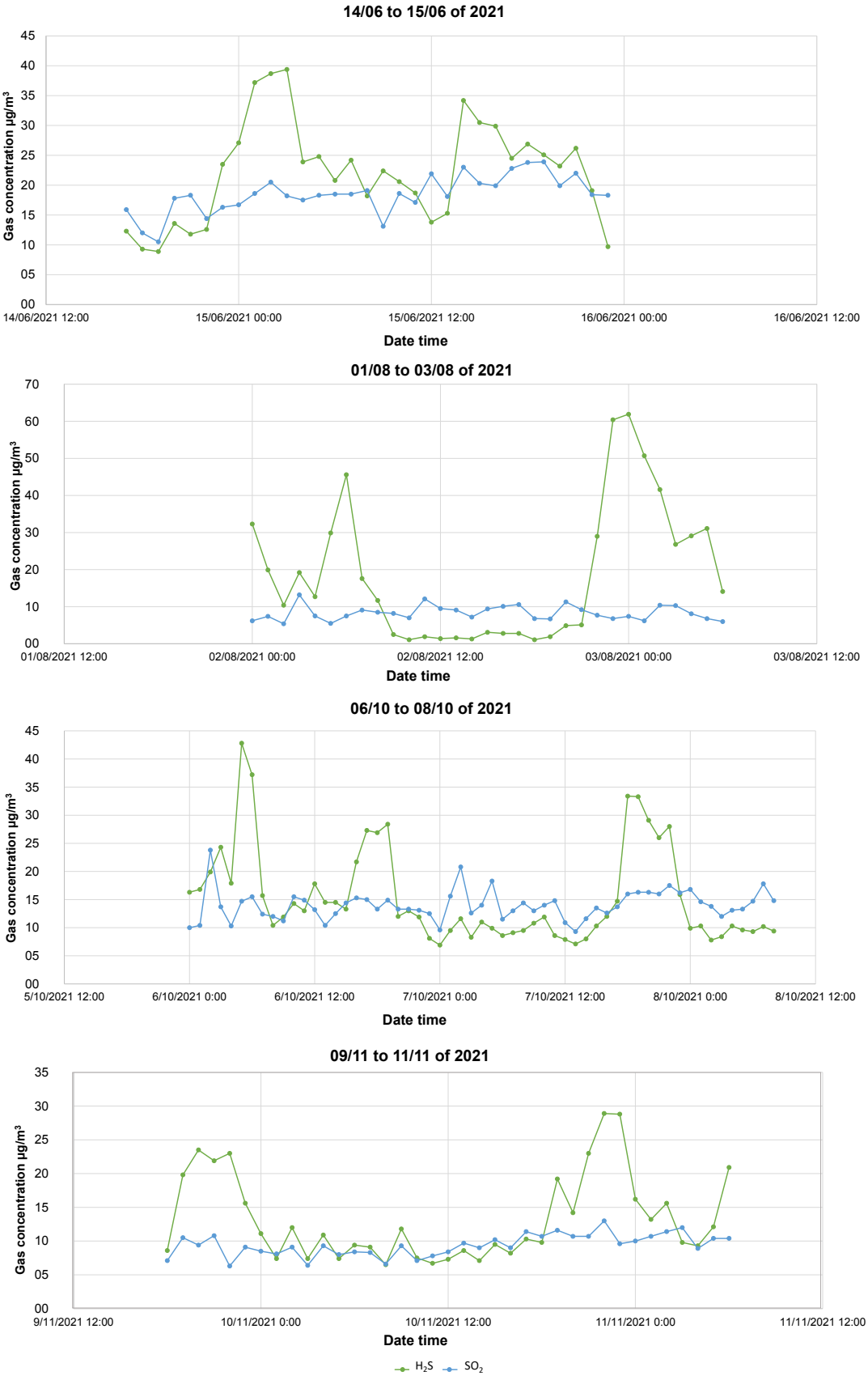

Figure 7: H_2S and SO_2 behaviour per hours in the specific coincident dates from surveys and Gwad'Air reports. These data include background values for both gas species.

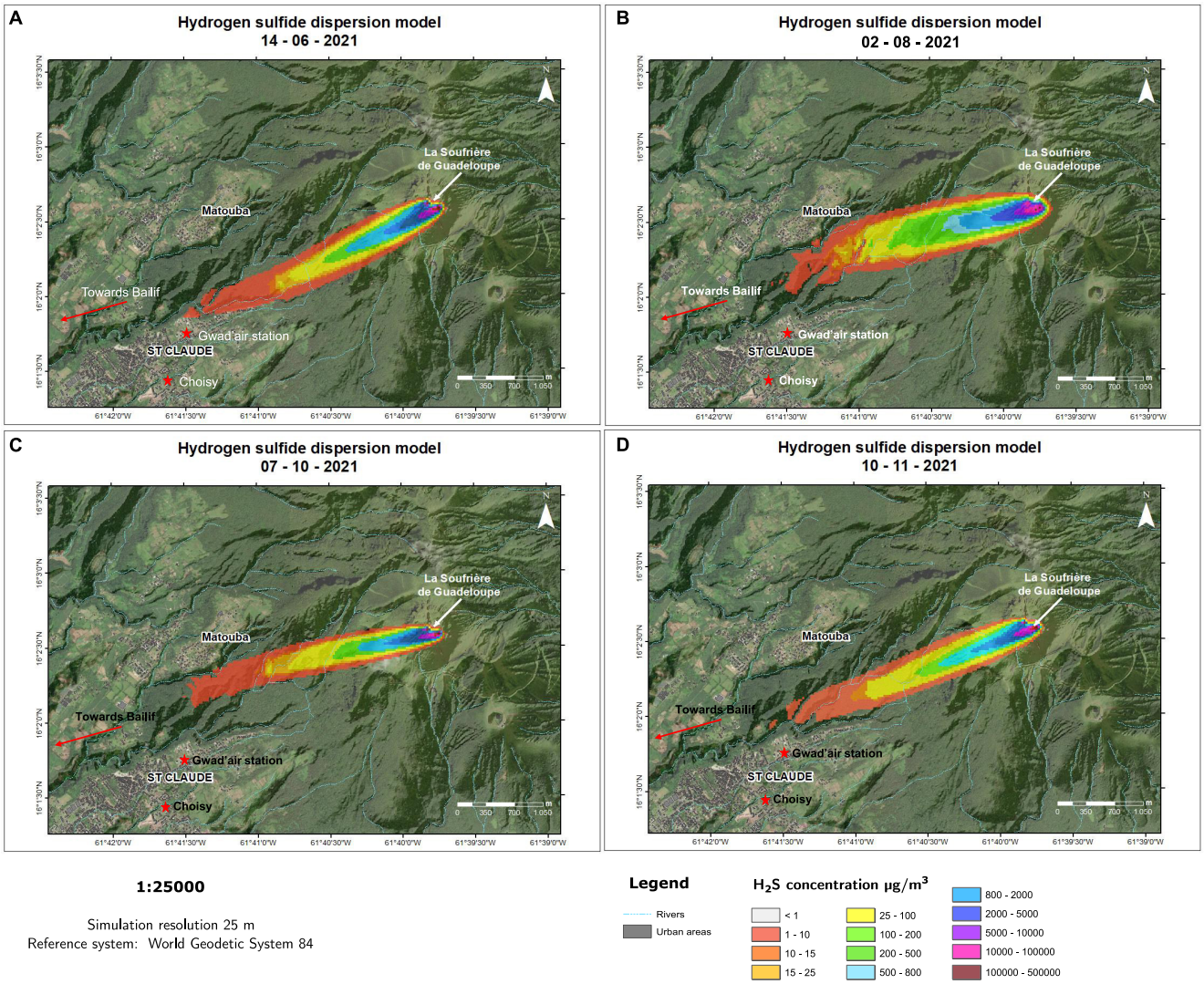

Figure 8: [A]–[D] Ground-level H_2S gas dispersion models for the report's dates with a highest H_2S concentration in St. Claude. Basemap from ESRI.

ference of less than 5 and 2 µg m^{-3} for the respective days simulated. The simulated gas plume does not quite reach the urban area of St. Claude in these cases. However, this is at a distance of no more than 1 km and the propagation of the gases is in the direction of the measurement and survey locations. In fact, in the 07-10-2021 simulation, although initially the gases disperse towards Matouba, the distal plume deviates towards the south which suggests that it could easily reach the north east of St. Claude. In addition, on 10-11-2021, the simulation suggests that the gases reach the periphery of St. Claude and is also in the direction of Baillif, the place where this date was reported in the surveys.

With these four tests above, we have shown that the values measured by Gwad'Air are within the range predicted by our simulations, demonstrating the power of the gas dispersion model as a tool to estimate the gas concentrations perceived by the populations around the volcano. Discrepancies regarding the exact dispersion direction or the precise gas concentration values may be due to the model resolution, an under- or over-estimation of gas fluxes, uncertainty in the meteorological conditions in those specific cases, and/or the non-conservative behaviour of H_2S that is not accounted for in the model. However, it is not our intention to model gas dispersion exactly for these cases, rather to highlight the good agreement between real measurements and the predictions of the simulations.

According to the Gwad'Air H_2S measurements , the average H_2S concentration in our selected dates are in the range of 4 to 20 µg m^{-3} (Table 2). These zones are no more than 1.5 km from the places where H_2S was measured (Gwad'Air station) or reported (Choisy sector). To account for this discrepancy, we would have to use a higher gas flux as input or to consider other factors in our models, such as the persistance, accumulation or contribution of gas emissions from the previous day, or other H_2S sources such as soil degassing or thermal springs. It is also important to consider that, in our simulations, the reported gas concentration is the average value over the entire 25 × 25 m pixel. Hence, the concentration at a particular location such as the Gwad'Air station could be higher than the simulations suggest.

The H_2S flux inputs for the simulations was an average measured in the month concerning each studied date. On days with high H_2S emissions, indicated both by the Gwad'Air station measurements and by the surveys from residents, the flux of gas from La Soufrière may have been larger than monthly average and, therefore, our simulations may underestimate the true gas concentrations. Furthermore, we note from the peaks in H_2S values measured by the Gwad'Air station (Figure 5), that some simulated days are preceded by days with high H_2S values. Given the strong winds at all locations in this study it does not seem likely that accumulation or persistence of gases could be an issue. Indeed, we took care to simulate sufficient time for the gas plume to fully arrive at the locations of interest.

Additionally, according to Allard et al. [2014], hydrothermal manifestations at La Soufrière, such as thermal springs and diffuse soil gas emanations, have also contributed to the volatile budget of the volcano. Their measurements from 2012 suggest a contribution of up to 4.5 % from the thermal springs around the lava dome and 2 % of H_2S as soil diffuse gas from the Faille de la Ty fault zone at the bottom of the dome. However, the thermal springs and the Faille de la Ty are not located near the fumarolic vents and their emanations will not contribute to the gas plume. Lastly, soil degassing from the top of La Soufrière close to the Napoléon Nord vent was measured to be equivalent to 2 % of the gas fumarolic output [Lebas 2021]. This is a negligible contribution to the overall degassing budget and thus unnecessary to include in our simulations.

5.4 Probability of H_2S exposure and its implications

5.4.1 *H_2S exposure quantification*

With our four tests above, we have shown that the values measured by Gwad'Air are within the range calculated by our simulations, therefore, we can consider our gas dispersion model as an accurate tool for determining gas levels in the surrounding areas of the volcano. From our CO_2 dispersion map (Figure 6B), we converted CO_2 values in H_2S concentrations using the average CO_2/H_2S molar ratio of 3.6 (Supplementary Material 2.A) and we plotted them as H_2S dispersion models (Figure 9). Based on Gwad'Air measurements, the average H_2S in St. Claude is 5 (± 0.25) µg m^{-3} (~3.5 ppb), which is concordance with the most probable simulated H_2S concentration in St. Claude of 1.4 to 4.6 ppb. Hence, based on our model simulations we determine that the H_2S concentration in Matouba is in the range 14–30 ppb (Figure 9).

Health effects related to H_2S exposure have been compiled by the World Health Organisation [2000]. According to this study, H_2S can be smelt by humans in concentrations from 0.008 ppm to 0.2 ppm (8–200 ppb). Health effects may occur from acute exposure to 2 ppm for the sensitive and asthmatic population or to 5 ppm for the general population. These values are at least three orders of magnitude higher than the H_2S concentration measured and simulated in Matouba or St. Claude. However, they are established for acute, short-term exposure (minutes to hours). Here, we aim to determine the exposure to gas emissions for permanent inhabitants of these towns, who are chronically exposed to gas emissions (weeks to years to lifetime exposure). Some low-concentration H_2S values have been established as references by toxicological and environmental agencies (e.g. United States Agency for Toxic Substances and Disease Registry) as guidelines to protect people from ambient H_2S in lifetime exposures. These guidelines consider both general and sensitive populations and they are given as recommended maximum concentrations for long-term exposure. For example, for a continuous lifetime exposure (24/7), the suggested maximum H_2S concentration is 1.5 ppb [U.S. EPA 2003]; for a long-term (i.e. 8 years) continuous exposure to H_2S, the reference value of is 8 ppb [CalOEHHA 2000]. Finally, continuous semi-accute exposure (up to 15 days) should not exceed 70 ppb H_2S [ATSDR 1999].

Based on these reference values and the calculated H_2S concentration in Matouba (14–30 ppb), the population there could be exceeding the maximum recommended H_2S concentration if they are exposed to continuous periods, longer than 8 years of more than 8 ppb H_2S. Moreover, for St. Claude (H_2S concentration values 1.4–4.6 ppb) the population could easily exceed the recommended limit for continuous lifetime exposure (1.5 ppb H_2S).

5.4.2 *Probabilistic H_2S maps*

To further quantify the above observations, and to establish realistic exposures for the populations of Matouba and St. Claude, we calculated the probability of exceeding the reference H_2S concentration values. Probability is the relation between the number of "favourable" events and total number of events. Hence for all points within the modelled domain, the probability of presenting a gas concentration, c, higher than a recommendable limit is:

> $P(c >$ threshold) = Number of simulations where concentration exceeds threshold / Total number of simulations.

We calculated probability maps for exceeding the 1.5, 8, and 70 ppb thresholds and show these in Figure 10. In all three cases, there is an 80–100 % chance of exceeding these thresholds within the first 1 km of the summit. Concerning the towns and villages downwind of the volcano, the probability of exceeding 1.5 ppb is 2–5 % in St. Claude (eastern sectors only) and 50–60 % in Matouba (Figure 10A). This means that, on average, the inhabitants of St. Claude are exposed to potentially harmful concentrations of H_2S on fewer than 18 days per year, whereas inhabitants of Matouba are exposed for more than half the year. We find that the eastern part of St. Claude has a probability of 2–5 % of exceeding the 8 ppb concentration threshold, though Figure 10B suggests that less of the town would be affected. This probability equates to around seven days per year, on average. However, in Matouba the probability of exceeding this value is around 40–50 %, which means approximately 145–180 days per year on average. We note that 8 ppb is the lowest concentration value at which H_2S odours can be perceived by humans [WHO 2000]. Therefore, it can be taken as a perception reference of the days when this limit value is being exceeded. Finally, the probability of exceeding 70 ppb in St. Claude is negligible except in the closest areas to the volcano. Matouba, however, has a non-negligible probability of 10–20 % of exceeding 70 ppb which

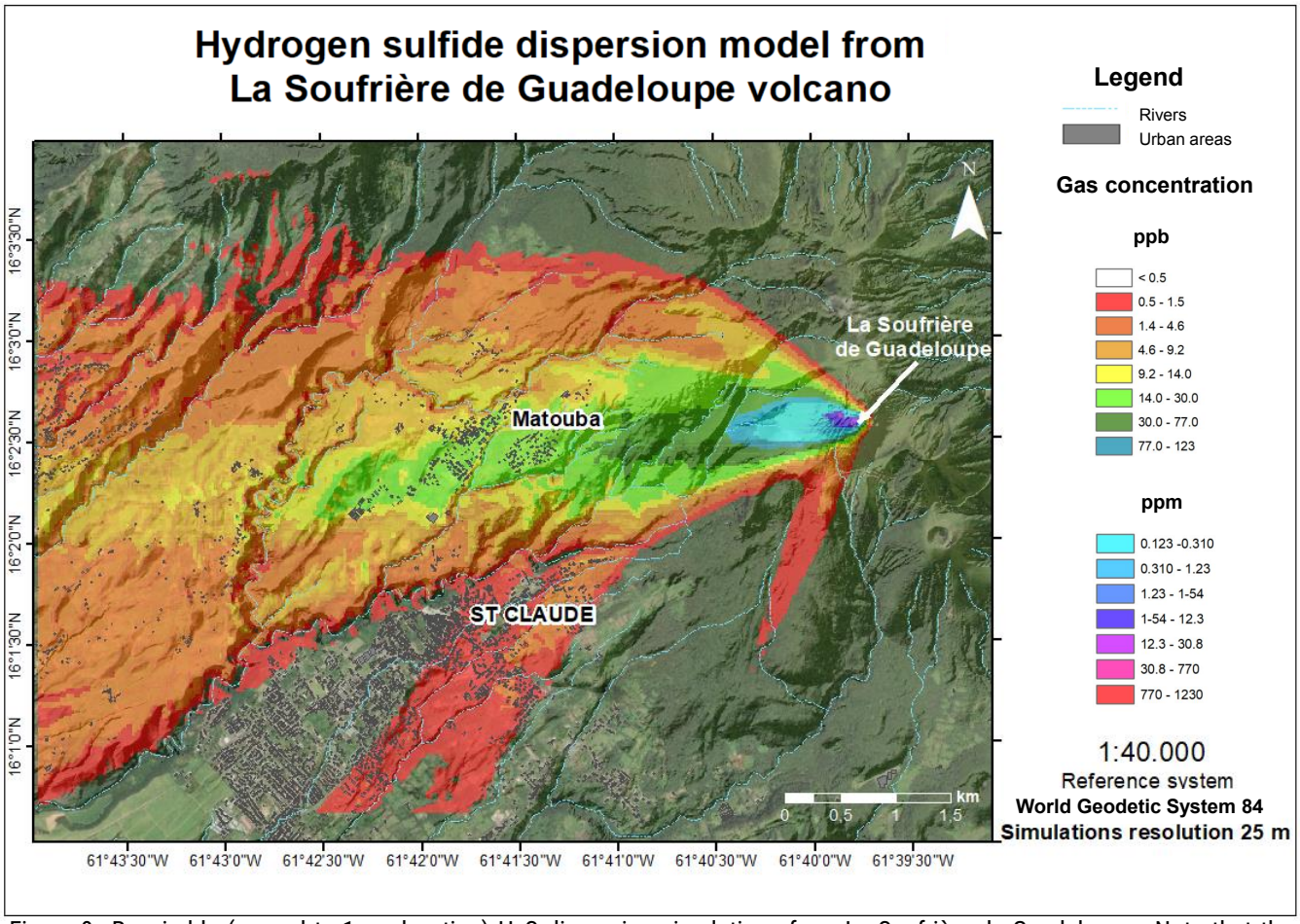

Figure 9: Respirable (ground to 1 m elevation) H_2S dispersion simulations from La Soufrière de Guadeloupe. Note that the apparent break in gas concentration scale at 123 ppb/0.123 ppm) accommodates the change in units at this value. Conversion coefficient used: H_2S ppb = H_2S µg m^{-3}/1.413. Basemap from ESRI.

represents 36–73 days per year. If this were to occur in a single, continuous exposure, such an event would exceed the recommendable H_2S exposure levels for the general (i.e. healthy) population [ATSDR 1999].

6 Conclusion

We ran ~100 gas dispersion simulations from La Soufrière de Guadeloupe volcano and calculated the most probable gas dispersion scenario for the surrounding region. The gas plume is dispersed westward, forming a fan emanating from the volcano summit and covering bearings of 255–270°. Gas concentration decreases rapidly westward. The highest concentrations are found in the centre of the dispersion fan. Gas concentrations are low in the distal fan borders. The zones where gases from La Soufrière are predominantly dispersed are Matouba and the uppermost peripheral areas of St. Claude.

We also ran four specific dates that coincided with days with H_2S odours that were reported by local inhabitants. We compared these simulations with the measured data of the Gwad'Air air quality station in St. Claude and found a high correspondence between the measured and simulated gas concentration values. Moreover, the calculated H_2S average in St. Claude measured by Gwad'Air is consistent with the range of values resulting from the simulations for that location. We therefore conclude that our gas dispersion model simulations are a reliable and powerful tool to estimate quantitative hazard assessment of gas exposure.

Based on the concentration maps produced from our simulations, we determined the volcanic gas exposure level in St. Claude and Matouba, and established the probability of harm to human health considering long-term continuous exposure (>8 years) to H_2S. We found the average volcanogenic H_2S concentration in St. Claude to be 3.5 ppb, and typically within the range of 1.4–4.6 ppb. In the case of Matouba, we found that the H_2S concentration was higher, within the range of 14–30 ppb. There is a probability of 2–5 % in St. Claude and 40–50 % in Matouba of exceeding 8 ppb of H_2S. This implies that, on average, there may be humanly-detectable levels of H_2S in St. Claude from 7–18 days in a year and 145–180 days in Matouba. A threshold of 70 ppb H_2S concentration is considered the most appropriate value for communities experiencing semi-acute exposure to H_2S (up to 15 days). In Matouba, the probability of exceeding this threshold is of 10–20 %, i.e. 36 to 73 days per year It this is taken to be a continuous period of days, there is a non-negligible probability for these populations of health issues due to the presence of volcanic gases.

Our gas dispersion maps could be used as a reference to establish and further study the possible risks related to these gas

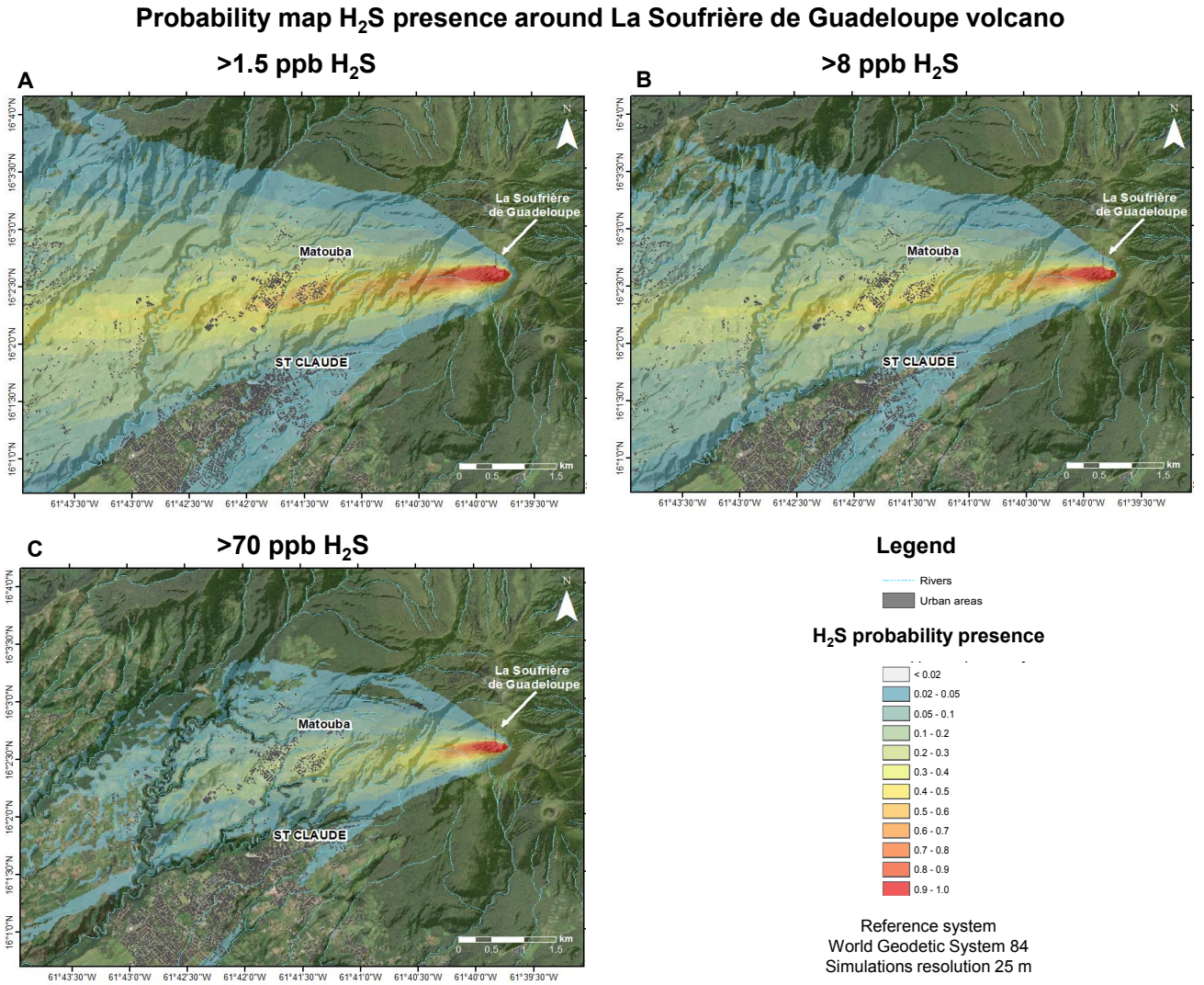

Figure 10: Probability maps for respirable (ground to 1 m elevation) H_2S presence around La Soufrière de Guadeloupe volcano. Reference values are from WHO guidelines.

exposure. Furthermore, the probability maps for H_2S exposure provide a powerful tool to determine prevention plans for human health, and also for the protection of flora and fauna in the nearby zones to the volcano.

Our results highlight that, whilst populations living downwind of degassing volcanoes may not be instantaneously exposed to harmful concentration levels of gas, semi-acute to chronic exposure to low concentrations may induce health issues in the long run. Indeed, depending on prevailing meteorological conditions (particularly wind direction and strength), human settlements may be regularly subject to concentration levels that exceed medically established guidelines for continuous low-level exposure.

Author Contributions

YPRB performed the numerical simulations, analysed datasets and prepared the manuscript. DEJ oversaw the numerical simulations and data analyses. SM performed the MG measurements and data processing. DEJ and SM supervised YPRB and prepared the manuscript. CG was responsible for the air-quality station installation and data acquisition. RM provided feedback on the project and prepared the manuscript. Gwad'Air technical service provided corrected air-quality data.

Acknowledgements

The authors are grateful to the Mésocentre Clermont Auvergne University for providing help, computing and storage resources. We also thank Thierry Hamel for assistance with computing resources. This work benefited from the French government initiative "Programme d'Investissements d'Avenir" managed by the Agence Nationale de la Recherche (ANR) under grant ANR-20-SFRI-0003 project CAP GS. This work was supported by the EU-funded project IMMERGE (Impact multi-environnemental des retombées volcaniques et sahariennes en Guadeloupe; PI: Céline Dessert, IPGP). This project has been financially supported by European (FEDER FSE PO 2014–2020) and Région Guadeloupe (agreement GP0023419)

funding. This study is LabEx ClerVolc contribution number 571. RM acknowledges OVSG-IPGP where this work started and where he was previously affiliated. The authors are grateful to F. Aguillera and two other anonymous reviewers for their comments that helped improve our manuscript, and to the editor C. Montagna for its handling.

Data Availability

Sanner meteorological and MultiGAS flux data are available from the OVSG WebObs service, on request (https://webobs.ovsg.univ-ag.fr/). ECWMF-ERA5 data are available through the Copernicus Climate Data Store portal (https://cds.climate.copernicus.eu/). Gwad'Air data are available from the authors upon request. DISGAS and DIAGNO are available from the INGV (http://datasim.ov.ingv.it/). The DEM and background images are available via the IGN's geoservices portal (https://geoservices.ign.fr/catalogue).

Copyright Notice

References

Agency for Toxic Substances and Disease Registry (ATSDR) (1999). *Toxicological Profile for Hydrogen Sulfide*. ATSDR, Altanta GA.

Aiuppa, A. (2005). "Chemical mapping of a fumarolic field: La Fossa Crater, Vulcano Island (Aeolian Islands, Italy)". *Geophysical Research Letters* 32(13). DOI: 10.1029/2005gl023207.

Allard, P., A. Aiuppa, F. Beauducel, D. Gaudin, R. Di Napoli, S. Calabrese, F. Parello, O. Crispi, G. Hammouya, and G. Tamburello (2014). "Steam and gas emission rate from La Soufriere volcano, Guadeloupe (Lesser Antilles): Implications for the magmatic supply during degassing unrest". *Chemical Geology* 384, pages 76–93. DOI: 10.1016/j.chemgeo.2014.06.019.

Baxter, P. J., R. E. Stoiber, and S. N. Williams (1982). "Volcanic gases and health: Masaya Volcano, Nicaragua". *The Lancet* 320(8290), pages 150–151. DOI: 10.1016/s0140-6736(82)91109-6.

Baxter, P. J., D. Tedesco, G. Miele, J. Baubron, and K. Cliff (1990). "Health hazards of volcanic gases". *The Lancet* 336(8708), page 176. DOI: 10.1016/0140-6736(90)91695-7.

Beauchamp, R. O., J. S. Bus, J. A. Popp, C. J. Boreiko, D. A. Andjelkovich, and P. Leber (1984). "A Critical Review of the Literature on Hydrogen Sulfide Toxicity". *CRC Critical Reviews in Toxicology* 13(1), pages 25–97. DOI: 10.3109/10408448409029321.

Boudon, G., J.-C. Komorowski, B. Villemant, and M. P. Semet (2008). "A new scenario for the last magmatic eruption of La Soufrière of Guadeloupe (Lesser Antilles) in 1530 A.D. Evidence from stratigraphy radiocarbon dating and magmatic evolution of erupted products". *Journal of Volcanology and Geothermal Research* 178(3), pages 474–490. DOI: 10.1016/j.jvolgeores.2008.03.006.

California Office of Environmental Health Hazard Assessment (CalOEHHA) (2000). *Chronic toxicity summary: hydrogen sulfide*. Technical report. Sacramento, CA: California EPA Office of Environmental Health Hazard Assessment.

Christenson, B., A. Reyes, R. Young, A. Moebis, S. Sherburn, J. Cole-Baker, and K. Britten (2010). "Cyclic processes and factors leading to phreatic eruption events: Insights from the 25 September 2007 eruption through Ruapehu Crater Lake, New Zealand". *Journal of Volcanology and Geothermal Research* 191(1-2), pages 15–32. DOI: 10.1016/j.jvolgeores.2010.01.008.

Cortis, A. and C. M. Oldenburg (2009). "Short-Range Atmospheric Dispersion of Carbon Dioxide". *Boundary-Layer Meteorology* 133(1), pages 17–34. DOI: 10.1007/s10546-009-9418-y.

Costa, A. and G. Macedonio (2016). *DISGAS-2.0: A model for passive DISpersion of GAS*. Rapporti tecnici 332. Istituto Nazionale di Geofisica e Vulcanologia.

D'Alessandro, W. (2006). "Gas hazard: an often neglected natural risk in volcanic areas". *Geo-Environment and Landscape Evolution II: Monitoring, Simulation, Management and Remediation*. WIT Press. DOI: 10.2495/geo060371.

Davis, J. B. and D. W. Kirkland (1979). "Bioepigenetic sulfur deposits". *Economic Geology* 74(2), pages 462–468. DOI: 10.2113/gsecongeo.74.2.462.

Dioguardi, F., S. Massaro, G. Chiodini, A. Costa, A. Folch, G. Macedonio, L. Sandri, J. Selva, and G. Tamburello (2022). "VIGIL: A Python tool for automatized probabilistic VolcanIc Gas dIspersion modeLling". *Annals of Geophysics* 65(1), page DM107. DOI: 10.4401/ag-8796.

Douglas, S. G., R. C. Kessler, and E. L. Carr (1990). *User's guide for the Urban Airshed Model. User's manual for the Diagnostic Wind Model*. Volume 3. PB-91-131243/XAB. Systems Applications, Inc., San Rafael, CA (USA).

Ewing, R. E. and H. Wang (2001). "A summary of numerical methods for time-dependent advection-dominated partial differential equations". *Journal of Computational and Applied Mathematics* 128(1-2), pages 423–445. DOI: 10.1016/s0377-0427(00)00522-7.

Feuillard, M., C. Allegre, G. Brandeis, R. Gaulon, J. L. Mouel, J. Mercier, J. Pozzi, and M. Semet (1983). "The 1975–1977 crisis of la Soufriere de Guadeloupe (F.W.I): A still-born magmatic eruption". *Journal of Volcanology and Geothermal Research* 16(3-4), pages 317–334. DOI: 10.1016/0377-0273(83)90036-7.

Feuillet, N., I. Manighetti, P. Tapponnier, and E. Jacques (2002). "Arc parallel extension and localization of volcanic complexes in Guadeloupe, Lesser Antilles". *Journal of Geophysical Research: Solid Earth* 107(B12), ETG 3–1–ETG 3–29. DOI: 10.1029/2001jb000308.

Fischer, T. P. and G. Chiodini (2015). "Volcanic, Magmatic and Hydrothermal Gases". *The Encyclopedia of Volcanoes*. Elsevier, pages 779–797. DOI: 10.1016/b978-0-12-385938-9.00045-6.

Gaudin, D., F. Beauducel, O. Coutant, C. Delacourt, P. Richon, J.-B. de Chabalier, and G. Hammouya (2016). "Mass and heat flux balance of La Soufrière volcano (Guadeloupe) from aerial infrared thermal imaging". *Journal of Volcanology and Geothermal Research* 320, pages 107–116. DOI: 10.1016/j.jvolgeores.2016.04.007.

Giggenbach, W. F. (1996). "Chemical Composition of Volcanic Gases". *Monitoring and Mitigation of Volcano Hazards*. Springer Berlin Heidelberg, pages 221–256. DOI: 10.1007/978-3-642-80087-0_7.

Granieri, D., A. Costa, G. Macedonio, M. Bisson, and G. Chiodini (2013). "Carbon dioxide in the urban area of Naples: Contribution and effects of the volcanic source". *Journal of Volcanology and Geothermal Research* 260, pages 52–61. DOI: 10.1016/j.jvolgeores.2013.05.003.

Guidotti, T. L. (2010). "Hydrogen Sulfide". *International Journal of Toxicology* 29(6), pages 569–581. DOI: 10.1177/1091581810384882.

Hersbach, H., B. Bell, P. Berrisford, S. Hirahara, A. Horányi, J. Muñoz-Sabater, J. Nicolas, C. Peubey, R. Radu, D. Schepers, A. Simmons, C. Soci, S. Abdalla, X. Abellan, G. Balsamo, P. Bechtold, G. Biavati, J. Bidlot, M. Bonavita, G. D. Chiara, P. Dahlgren, D. Dee, M. Diamantakis, R. Dragani, J. Flemming, R. Forbes, M. Fuentes, A. Geer, L. Haimberger, S. Healy, R. J. Hogan, E. Hólm, M. Janisková, S. Keeley, P. Laloyaux, P. Lopez, C. Lupu, G. Radnoti, P. de Rosnay, I. Rozum, F. Vamborg, S. Villaume, and J.-N. Thépaut (2020). "The ERA5 global reanalysis". *Quarterly Journal of the Royal Meteorological Society* 146(730), pages 1999–2049. DOI: 10.1002/qj.3803.

Hill, F. B. (1973). "Atmospheric sulfur and its links to the biota". *Carbon and the biosphere: proceedings of the 24th Brookhaven Symposia in Biology*. Volume 24, pages 159–181. ISBN: 0-87079-006-4.

Jessop, D. E., S. Moune, R. Moretti, D. Gibert, J.-C. Komorowski, V. Robert, M. J. Heap, A. Bosson, M. Bonifacie, S. Deroussi, C. Dessert, M. Rosas-Carbajal, A. Lemarchand, and A. Burtin (2021). "A multi-decadal view of the heat and mass budget of a volcano in unrest: La Soufrière de Guadeloupe (French West Indies)". *Bulletin of Volcanology* 83(3). DOI: 10.1007/s00445-021-01439-2.

Komorowski, J.-C., G. Boudon, F. Michel-Semet Beauducel, C. Anténor-Habazac, S. Bazin, and G. Hammouya (2005). "Guadeloupe". *Volcanic Atlas of the Lesser Antilles*. Edited by J. M. Lindsay, R. E. A. Robertson, J. B. Shepherd, and S. Ali. St. Augustine, Trinidad and Tobago: Seismic Research Unit, The University of the West Indies, pages 67–106. ISBN: 976-95142-0-9.

Lebas, F. (2021). "Etude du dégazage et de la perte de chaleur du système hydrothermal de La Soufrière de Guadeloupe : implications pour la surveillance volcanique". Master's thesis. Université de Paris-IPGP.

Massaro, S., F. Dioguardi, L. Sandri, G. Tamburello, J. Selva, S. Moune, D. E. Jessop, R. Moretti, J.-C. Komorowski, and A. Costa (2021). "Testing gas dispersion modelling: A case study at La Soufrière volcano (Guadeloupe, Lesser Antilles)". *Journal of Volcanology and Geothermal Research* 417, page 107312. DOI: 10.1016/j.jvolgeores.2021.107312.

Metcalfe, A., S. Moune, J.-C. Komorowski, G. Kilgour, D. E. Jessop, R. Moretti, and Y. Legendre (2021). "Magmatic Processes at La Soufrière de Guadeloupe: Insights From Crystal Studies and Diffusion Timescales for Eruption Onset". *Frontiers in Earth Science* 9. DOI: 10.3389/feart.2021.617294.

Moretti, R., I. Arienzo, L. Civetta, G. Orsi, and P. Papale (2013). "Multiple magma degassing sources at an explosive volcano". *Earth and Planetary Science Letters* 367, pages 95–104. DOI: 10.1016/j.epsl.2013.02.013.

Moretti, R., J.-C. Komorowski, G. Ucciani, S. Moune, D. Jessop, J.-B. de Chabalier, F. Beauducel, M. Bonifacie, A. Burtin, M. Vallée, S. Deroussi, V. Robert, D. Gibert, T. Didier, T. Kitou, N. Feuillet, P. Allard, G. Tamburello, T. Shreve, J.-M. Saurel, A. Lemarchand, M. Rosas-Carbajal, P. Agrinier, A. L. Friant, and M. Chaussidon (2020). "The 2018 unrest phase at La Soufrière of Guadeloupe (French West Indies) andesitic volcano: Scrutiny of a failed but prodromal phreatic eruption". *Journal of Volcanology and Geothermal Research* 393, page 106769. DOI: 10.1016/j.jvolgeores.2020.106769.

Moretti, R., S. Moune, D. Jessop, C. Glynn, V. Robert, and S. Deroussi (2021). "The Basse-Terre Island of Guadeloupe (Eastern Caribbean, France) and Its Volcanic-Hydrothermal Geodiversity: A Case Study of Challenges, Perspectives, and New Paradigms for Resilience and Sustainability on Volcanic Islands". *Geosciences* 11(11), page 454. DOI: 10.3390/geosciences11110454.

Moune, S., R. Moretti, A. Burtin, D. E. Jessop, T. Didier, V. Robert, M. Bonifacie, G. Tamburello, J.-C. Komorowski, P. Allard, and M. Buscetti (2022). "Gas Monitoring of Volcanic-Hydrothermal Plumes in a Tropical Environment: The Case of La Soufrière de Guadeloupe Unrest Volcano (Lesser Antilles)". *Frontiers in Earth Science* 10. DOI: 10.3389/feart.2022.795760.

Observatoire volcanologique et sismologique de la Guadeloupe-Institut de physique du globe de Paris (1999–2022). *Monthly reports on the activity of La Soufrière de Guadeloupe and on regional seismicity*. URL: http://www.ipgp.fr/fr/ovsg/bulletins-mensuels-de-lovsg (visited on 10/17/2023).

Oppenheimer, C., B. Scaillet, and R. S. Martin (2011). "Sulfur Degassing From Volcanoes: Source Conditions, Surveillance, Plume Chemistry and Earth System Impacts". *Reviews in Mineralogy and Geochemistry* 73(1), pages 363–421. DOI: 10.2138/rmg.2011.73.13.

Pareschi, M. T., M. Ranci, M. Valenza, and G. Graziani (1999). "The assessment of volcanic gas hazard by means of numerical models: An example from Vulcano Island (Sicily)". *Geophysical Research Letters* 26(10), pages 1405–1408. DOI: 10.1029/1999gl900248.

Pedone, M., D. Granieri, R. Moretti, A. Fedele, C. Troise, R. Somma, and G. D. Natale (2017). "Improved quantification of CO_2 emission at Campi Flegrei by combined Lagrangian Stochastic and Eulerian dispersion modelling". *Atmospheric Environment* 170, pages 1–11. DOI: 10.1016/j.atmosenv.2017.09.033.

Rye, R. O. (2005). "A review of the stable-isotope geochemistry of sulfate minerals in selected igneous environments and related hydrothermal systems". *Chemical Geology* 215(1-4), pages 5–36. DOI: 10.1016/j.chemgeo.2004.06.034.

Rye, R. O., P. M. Bethke, and M. D. Wasserman (1992). "The stable isotope geochemistry of acid sulfate alteration". *Economic Geology* 87(2), pages 225–262. DOI: 10.2113/gsecongeo.87.2.225.

Shinohara, H. (2005). "A new technique to estimate volcanic gas composition: plume measurements with a portable multi-sensor system". *Journal of Volcanology and Geothermal Research* 143(4), pages 319–333. DOI: 10.1016/j.jvolgeores.2004.12.004.

Symonds, R., T. Gerlach, and M. Reed (2001). "Magmatic gas scrubbing: implications for volcano monitoring". *Journal of Volcanology and Geothermal Research* 108(1-4), pages 303–341. DOI: 10.1016/s0377-0273(00)00292-4.

Tamburello, G. (2015). "Ratiocalc: Software for processing data from multicomponent volcanic gas analyzers". *Computers &amp Geosciences* 82, pages 63–67. DOI: 10.1016/j.cageo.2015.05.004.

Tamburello, G., S. Moune, P. Allard, S. Venugopal, V. Robert, M. Rosas-Carbajal, S. Deroussi, G.-T. Kitou, T. Didier, J.-C. Komorowski, F. Beauducel, J.-B. De Chabalier, A. Le Marchand, A. Le Friant, M. Bonifacie, C. Dessert, and R. Moretti (2019). "Spatio-Temporal Relationships between Fumarolic Activity, Hydrothermal Fluid Circulation and Geophysical Signals at an Arc Volcano in Degassing Unrest: La Soufrière of Guadeloupe (French West Indies)". *Geosciences* 9(11), page 480. DOI: 10.3390/geosciences9110480.

Textor, C., H.-F. Graf, C. Timmreck, and A. Robock (2004). "Emissions from volcanoes". *Advances in Global Change Research*. Springer Netherlands, pages 269–303. DOI: 10.1007/978-1-4020-2167-1_7.

Tortini, R., S. van Manen, B. Parkes, and S. Carn (2017). "The impact of persistent volcanic degassing on vegetation: A case study at Turrialba volcano, Costa Rica". *International Journal of Applied Earth Observation and Geoinformation* 59, pages 92–103. DOI: 10.1016/j.jag.2017.03.002.

Turner, J. S. (1979). *Buoyancy effects in fluids*. 2nd Edition. Cambridge university press. ISBN: 9780521297264.

U.S. Environmental Protection Agency (U.S. EPA) (2003). *IRIS record for hydrogen sulfide*. Technical report. U.S. Environmental Protection Agency.

Viveiros, F., E. Baldoni, S. Massaro, M. Stocchi, A. Costa, S. Caliro, G. Chiodini, and C. Andrade (2023). "Quantification of CO2 degassing and atmospheric dispersion at Caldeiras da Ribeira Grande (São Miguel Island, Azores)". *Journal of Volcanology and Geothermal Research* 438, page 107807. DOI: 10.1016/j.jvolgeores.2023.107807.

Williams-Jones, G. and H. Rymer (2015). "Hazards of Volcanic Gases". *The Encyclopedia of Volcanoes*. Edited by H. Sigurdsson, B. Houghton, S. R. McNutt, H. Rymer, and J. Stix. Elsevier, pages 985–992. DOI: 10.1016/b978-0-12-385938-9.00057-2.

World Health Organization (WHO) (2000). *Air quality guidelines for Europe*. 2nd edition. World Health Organization, Regional Office for Europe.